Seismoelectric effects for geothermal resources assessment and monitoring

Christina Morency, Eric Matzel, Niels Grobbe, Daniel Brito, Clarisse Bordes, Mathieu Bellanger, Mathieu Auxiètre, Kirsti Midttømme, Walter Wheeler, Hélène Barucq, et al.

Seismoelectric effects for geothermal resources assessment and monitoring

Christina Morency and Eric Matzel, Lawrence Livermore National Laboratory; Niels Grobbe, University of Hawai'i at Mānoa; Daniel Brito and Clarisse Bordes, Université de Pau et des Pays de l'Adour, LFCR; Hélène Barucq and Julien Diaz, INRIA; Mathieu Bellanger and Mathieu Auxiètre, TLS Geothermics; Kirsti Midttømme, Walter Wheeler and Roman Berenblyum, NORCE Norwegian Research Center AS; Bjarte Fagerås, OCTIO Environmental Monitoring*

Summary

In the context of geothermal power plant operations, large amount of fluid is injected and circulates through the subsurface. Being able to identify pre-existing water-filled fracture networks (reservoir scale) can greatly help to (1) image and assess geothermal resources and targets, and (2) inform on and monitor stimulation successes and risk mitigation, by mapping newly activated fracture networks. Traditional seismic imaging techniques fail to resolve fluid-phase properties, while purely electromagnetic approaches typically provide limited, low-resolution constraints on the rock structure. Our goal is to assess the use of seismoelectric effects (SEE), which arise from seismic-to-electromagnetic conversion in naturally charged porous media with a certain degree of fluid saturation. The key here is that, by leveraging the depth sensitivity of seismic signals, in combination with the fluid sensitivity of electromagnetic techniques, we can identify coupled seismic-EM pore-level phenomena and gain the advantages of both. In this contribution, we demonstrate the numerical implementation of SEE and highlight the existence of three type of signals. We also introduce in progress efforts of practical use of SEE for geothermal monitoring through laboratory experiments and field surveys.

Introduction

Imaging and monitoring of geothermal resources rely predominantly on seismic techniques, using acoustic or elastic rheology, which alone do not capture fluid properties and related mechanisms. Even a full poroelastic approach does not allow efficient resolution, or direct sensitivity, of fluid properties (Morency et al., 2011). This is in part because seismic sensors measure solid displacements and offer no direct constraints on the fluid. On the other hand, EM measurements add constraints to the fluid phase properties, such as resistivity and permeability, with little sensitivity to the solid phase. There have been efforts to combine seismic and EM data for exploration geophysics (e.g., Hoversten et al., 2006; Hu et al., 2009). The most popular approach is based on joint inversion of decoupled seismic (acoustic or elastic rheology) and EM datasets (e.g., Colombo and De Stefano, 2007), which are combined artificially through a common structural or petrophysical framework with arbitrary data weights indicating the relative importance of the two independent data sets, whereby each dataset is furthermore triggered by separate sources, seismic and electric, respectively, adding to deployment cost as well as to lack of source-reproducibility. In this case, the naturally coupled nature of seismic and EM phenomena is neglected, as seismoelectric effects are not modeled.

Seismoelectric effects are pore-scale phenomena relying on electric charge separation created by streaming currents generated by pressure gradients, which occur when a seismic wave propagates (Ivanov, 1939). This defines seismic-to-electric conversion. As illustrated in Figure 1, the propagating seismic wave generates an electrical current, which in turn induces an electrical field. This electrical field is often referred to as a coseismic field, propagating with the seismic wave. When this coseismic field is disrupted by a heterogeneity (due to e.g., a mechanical, electrical, or pore-fluid contrast), an electric dipole is created, triggering an independently diffusing EM field that is instantaneously detectable and provides information at depth, and is referred to as the so-called interface response field.

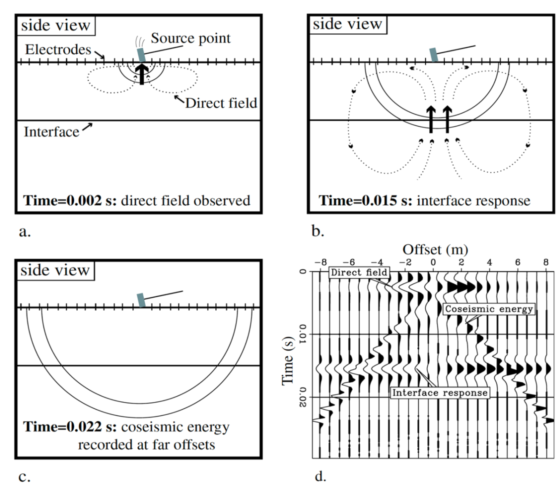

Figure 1: Schematic representation of seismoelectric survey and corresponding synthetic data. Panels (a), (b), and (c) show the propagation of the seismic wave. Note that in (c) the reflected seismic wave at the interface is neglected for simplicity. Corresponding SEE dataset, i.e., electric field, is plotted on panel (d), showing a direct field, interface response, and coseismic field (after Haines, 2004).

Seismoelectric effects for geothermal resources assessment and monitoring

Theory

Modeling of the seismoelectric effects relies upon the governing equations derived by Pride (1994), and subsequent modifications and improvements of its petrophysical relationships, corresponding to Biot's poroelastic wave equations (Biot 1956a, 1956b) and Maxwell's electromagnetic wave equations coupled electrokinetically. These coupled wave equations are solved here using a spectral-element method (SEM). The SEM, in contrast to finite-element methods (FEM) uses high-degree Lagrange polynomials. Not only does this allow the technique to handle complex geometries similarly to FEM, but it also retains exponential convergence and accuracy due to the use of high-degree polynomials (Komatitsch and Vilotte, 1998; Komatitsch and Tromp, 1999).

Numerical modeling

We have performed preliminary SEE forward simulations for carbon storage monitoring to assess the numerical implementation. In the context of carbon storage monitoring, we mimicked a cross-well monitoring setup in a homogenous porous medium, with a seismic source located in well A, and a series of collocated geophones and electrodes to record seismic displacement and associated, coupled electric fields, respectively, located in well B.

Following the trigger of a seismic source at depth, with a dominant frequency of 200 Hz, we display in Figure 2-a the modeled wave fronts at different times of:

- the seismic field, and
- the triggered coseismic electric field, which propagates at the same speed as the seismic field and is due to local fluid flow generated by the passage of the seismic wave.

In Figure 2-b (top), we plot the corresponding recorded vertical seismic displacement and electric field propagating in this baseline medium. We can see the compressional P-wave at the geophones, and the coseismic electric signal. We also detect a quasi-instantaneous electric signal generated at the time when the seismic source is triggered, which is the so-called source-converted seismoelectric EM field.

We then mimic the intrusion of CO_2 in the initially homogenous porous medium, saturated with brine (see Figure 2-b bottom). The records at the geophones show again a seismic P-wave, slightly delayed due to the presence of CO_2. However, electric waveforms recorded at the electrodes not only show coseismic and source triggered electrical signals like in the baseline case, but also display another, quasi-instantaneous seismoelectric conversion at the interface between the brine and the CO_2 saturation front.

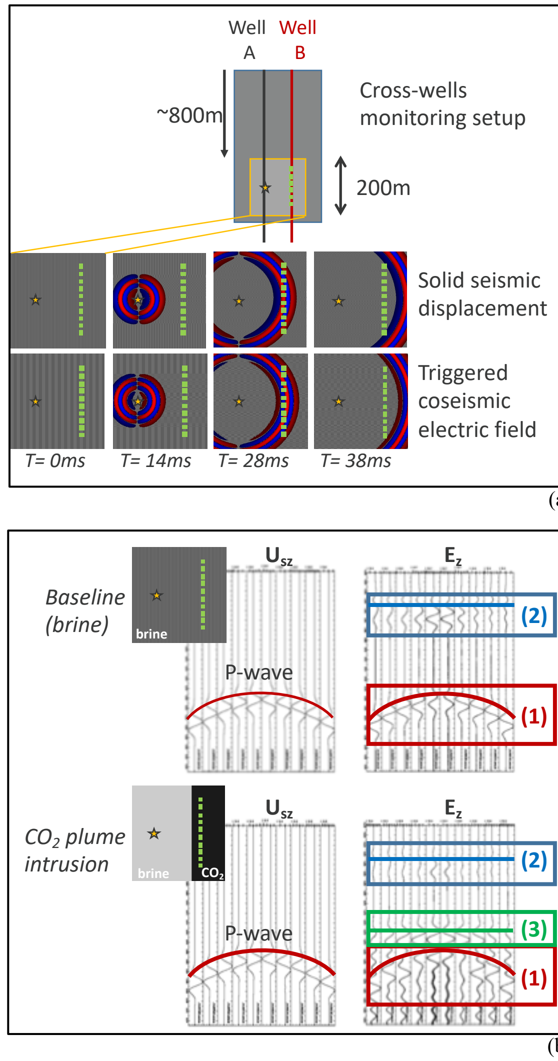

Figure 2: (a) Geometry of the cross-well monitoring setup, and snapshots of the horizontal seismic displacement and coseismic electric field. The yellow star refers to the seismic source location and the green squares correspond to the collocations of the geophones and electrodes. (b) Vertical seismic and electric waveforms recorded at the collocated geophones and electrodes, respectively, after propagation in a homogeneous porous medium saturated with brine as baseline (top) and after intrusion of CO_2 (bottom). The recorded seismic signals correspond to the compressional P-wave. The recorded electric signals correspond to (1) coseismic electric signal, (2) quasi-instantaneous electric signal generated when the seismic source occurs, and (3) quasi-instantaneous interface response.

Seismoelectric effects for geothermal resources assessment and monitoring

Laboratory experiments

Leveraging the development for the past decades of original and innovative experiments for the characterization of porous media (Bordes et al., 2006, 2008, 2015; Holzhauer et al., 2015; Devi et al., 2018), aiming at observing the effect of petrophysical properties (porosity, permeability, saturation) on mechanical and electromagnetic wave propagation, we are able to design a new set of experiments to specifically target SEE, which is in this context a hybrid seismic-EM experiment. Figure 3 shows a schematic representation of the SEE experimental setup.

With this setup, using material properties close to geothermal rocks, we test the influence of physical parameters (e.g., temperature, salinity, permeability) on the SEE signal in the context of geothermal prospection, validate our numerical method, and inform the optimal design of field surveys.

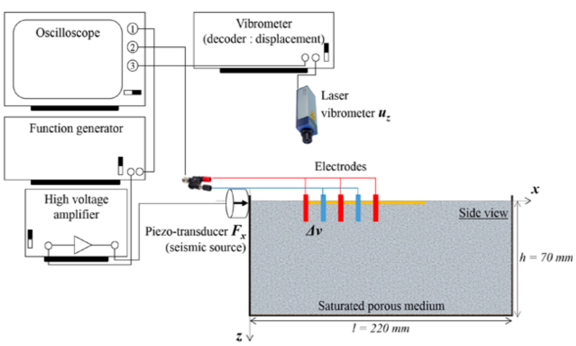

Figure 3: Schematic representation of a SEE experiment (Devi et al., 2018). An acoustic wave generated by a piezoelectric transducer propagates within saturated sand in a box of 22 cm length. Vertical electrodes buried in the sand measure the travelling coseismic SEE while a laser interferometer (top) measures the seismic wave at the top of the sand.

Field deployment

To show the practical use of SEE for geothermal assessment and monitoring, as a proof of concept we are targetting a geothermal site located in France and operated by TLS Geothermics since 2017. Geothermal exploration analysis based on field surveys and modeling were carried out between 2015 and 2018 using geological, geochemical, and geophysical acquisitions using magnetotelluric, gravity, and passive seismic methods (Figure 4). This led to the identification of a favorable geothermal prospect hosted in a granitic fault zone. A deep drilling is planned for 2021 with a target at 3500 m depth. A shallow 200 m deep well will also be drilled close by and will carry SEE instrumentation.

The approach is to use not only the local microseismicity as a source to the SEE signals but also the drill used during the deep drilling, which will act as a seismic source. Figure 5 shows a map view of the site with the position of the planned shallow well as well as a resistivity log, microseismicity, and faults structure.

Conclusions

We successfully numerically implemented seismic-to-electric conversion, which allows us to model SEE signals, characterized by a coseismic electric signal, a quasi-instantaneous electric signal generated by the seismic source, and a quasi-instantaneous interface response.

SEE sensitivity to a geothermal environment can be tested experimentally and inform on the optimal field deployment planned to demonstrate the practical use of SEE for geothermal monitoring.

Finally, although the signal-to-noise ratio of the converted seismic-to-electric signals can be challenging, SEE dataset can capture unique information on geothermal reservoir properties and heterogeneities, such as resistivity, salinity, degree of saturation and viscosity (e.g., Smeulders et al., 2014), as opposed to purely seismic or purely electromagnetic records. Lastly, SEE interface response fields created at changes in properties can detect thin layers and other fine-scaled structural features such as fractures beyond the seismic resolution (e.g., Grobbe and Slob, 2016).

Acknowledgements

This project has been subsidized through the Cofund GEOTHERMICA by the U.S. Department of Energy (DOE), Office of Energy Efficiency and Renewable Energy, under Contract DE-AC52-07NA27344 with Lawrence Livermore National Laboratory, by the French Environment and Energy Management Agency (ADEME), and by the Research Council of Norway. LLNL-PROC-821051

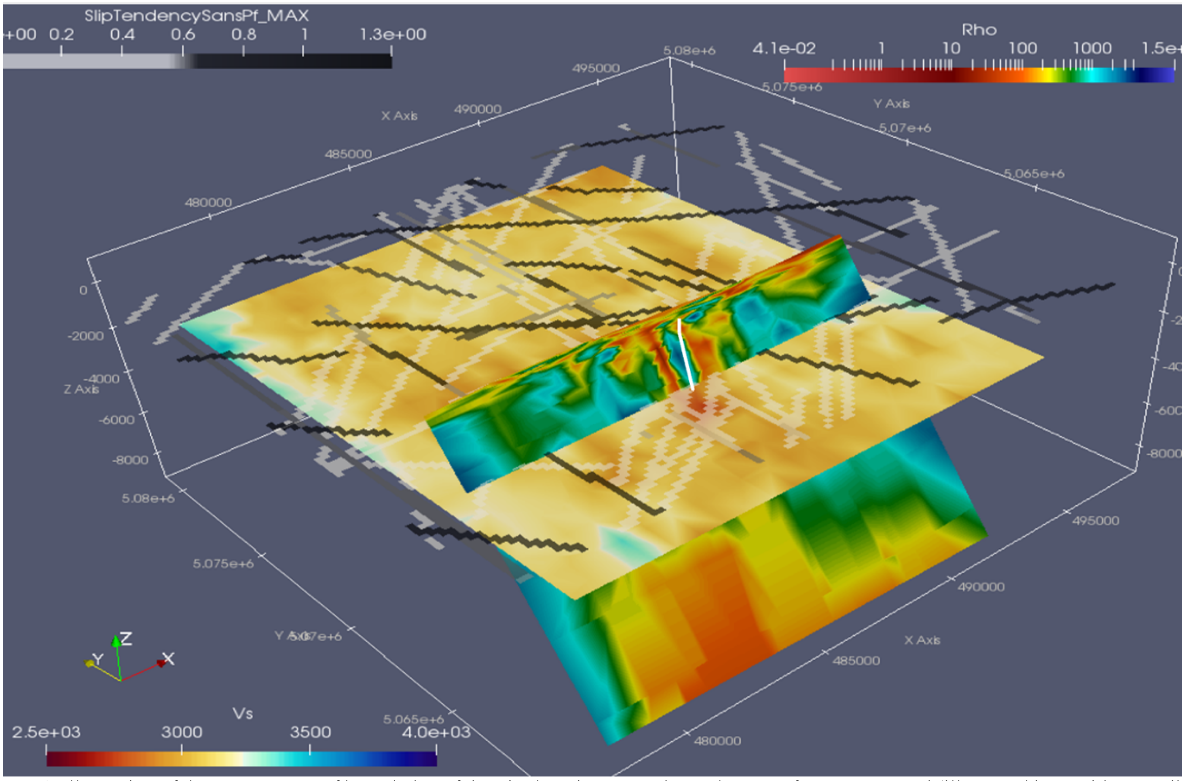

Figure 4: Illustration of the current state of knowledge of the Sioule-Miouze geothermal system from a structural (illustrated here with a possible slip tendency), electrical resistivity (Rho) and shear wave velocity (Vs) point of view. The expected deep drilling is illustrated by the white line. A shallow drilling will be located close to this deep drilling and carry SEE instrumentation.

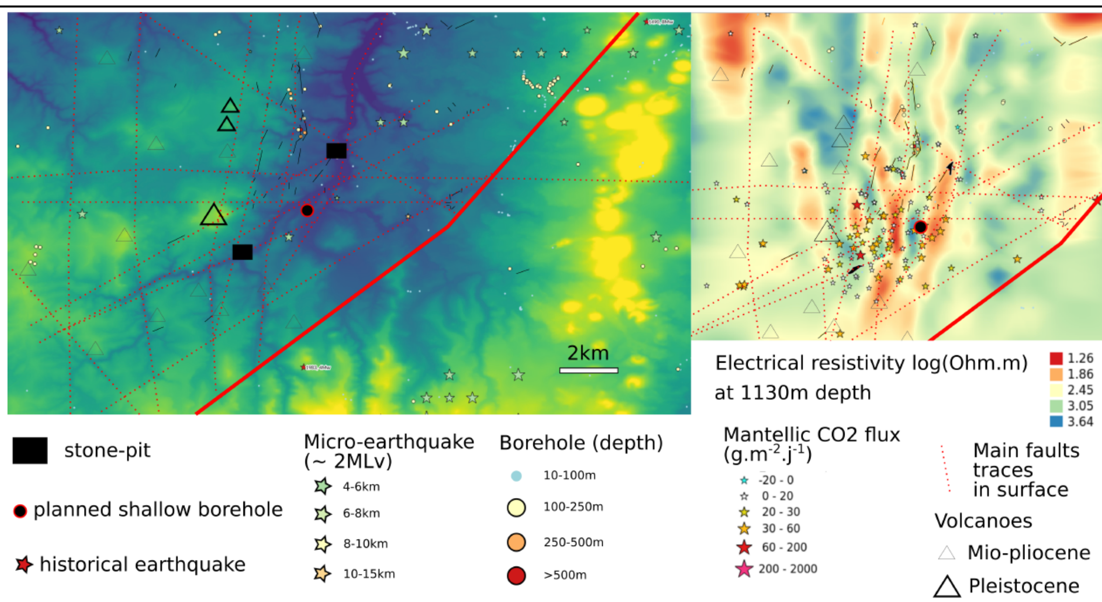

Figure 5: Map view of the Sioule-Miouze field test with microseismicity, main faults, and electrical resistivity.